Article
Vol. 25, No. 6, p. 749–762, December 2021
https://doi.org/10.1007/s12303-021-0008-4
pISSN 1226-4806 eISSN 1598-7477
Geosciences Journal GJ

Tidally-influenced deposition and microfacies sequences of fluid muds: Early Cretaceous McMurray Formation, Alberta, Canada

Juhyeon Oh and Hyung Rae Jo*

Department of Earth and Environmental Sciences, Andong National University, Andong, Gyeongsangbuk-do 36729, Republic of Korea

ABSTRACT: Fluid muds are common in estuarine environments, but their ancient examples have rarely been documented due to poor comprehension of their depositional processes and characteristics. Mudstone layers in the tidally-influenced channel sequences of the middle McMurray Formation are examined in detail through microscopic observations and interpreted on the basis of recent advances in the understanding of flow dynamics of high mud-concentration flows. The mudstone layers, < 1 to 25 mm thick, are classified into three microfacies. Structureless mudstone (Microfacies 1) consists mainly of clay particles with randomly dispersed coarse grains (coarse silt to fine sand). It represents cohesive mud flows with sufficient cohesive forces to support coarse grains (quasi-laminar plug flow). Silt-streaked mudstone (Microfacies 2) is similar to Microfacies 1 in texture, but contains discontinuous streaks of coarse-silt to very-fine-sand grains. It is interpreted as being also deposited by cohesive fluid muds. The silt streaks are, however, suggestive of the presence of weak turbulence under the cohesive plug (upper transitional plug flow). Heterolithic laminated mudstone (Microfacies 3) is characterized by alternations of very thin, silt and clay laminae, which are either parallel or low-angle cross-laminated. It is interpreted as the deposits of low-amplitude bed-waves formed in lower transitional plug flows. These microfacies reflect a range of flow phases of fluid muds, which changed as flow velocities and suspended sediment concentrations fluctuated with tidal cycles. Repeated vertical changes of microfacies are suggestive of an ideal sequence of fluid muds formed during tidal acceleration and deceleration. The sequence comprising microfacies 3, 2 and 1 in ascending order represents deposition from lower transitional plug flows through upper transitional plug flows to quasi-laminar plug flows as suspended sediment concentrations increase with flow deceleration. That of the reversed order of microfacies reflects the reversed change in flow types during acceleration. These results provide the basis for recognizing fluid-mud deposits and tidal signatures in ancient estuarine sequences.

Key words: fluid muds, high mud-concentration flows, mudstone microfacies, depositional processes, tidally-influenced deposition, McMurray Formation

Manuscript received November 2, 2020; Manuscript accepted April 19, 2021

1. INTRODUCTION

Fluid mud is defined as a high-concentration aqueous suspension of fine-grained sediment with a solid concentration in excess of 10 gL^{-1} (Ross and Mehta, 1989; McAnally et al., 2007). Estuarine environments contain large amounts of suspended fine sediments supplied from both rivers and seas. These fine sediments show a maximum concentration at the mixing zone of fresh water and sea water, where flocs of clay particles rapidly settle down and form fluid muds on the bottom (Kirby and Parker, 1983; Dalrymple and Choi, 2007; McAnally et al., 2007). Despite the common occurrence of fluid muds in recent estuarine environments, they have been rarely documented in ancient estuarine successions (e.g., Ichaso and Dalrymple, 2009; Mackay and Dalrymple, 2011). This is mainly due to poor understanding of the depositional processes and the products of high mud-concentration flows.

Recently experimental studies have increased knowledge on the dynamics of high mud-concentration flows (Baas and Best, 2002; Baas et al., 2009, 2011; Sumner et al., 2009). These experimental studies have shown that the flows with high mud concentrations gradually change from turbulent flows through transitional plug flows to quasi-laminar plug flows as suspended

*Corresponding author:
Hyung Rae Jo
Department of Earth and Environmental Sciences, Andong National University, 1375, Gyeongdong-ro, Andong, Gyeongsangbuk-do 36729, Republic of Korea
Tel: +82-54-820-5022, Fax: +82-54-822-5467, E-mail: hrjo@anu.ac.kr

sediment concentrations increase. Five flow types are distinguished in the flow transition, based on turbulence intensity and the development of a cohesive plug: turbulent flow (TF), turbulence-enhanced transitional flow (TETF), lower transitional plug flow (LTPF), upper transitional plug flow (UTPF) and quasi-laminar plug flow (QLPF) (Fig. 1). With an increase in mud concentrations in turbulent flows, turbulence intensity increases across the entire flow depth due to the generation of strong turbulence close to the bed (TETF). A further increase in mud concentrations results in the formation of a cohesive plug overlying a lower region of high velocity gradient and strong turbulence (LTPF). Turbulence intensity in the lower region increases until the flow reaches an upper transitional plug flow. The cohesive plug expands downwards with increasing mud concentrations, and turbulence intensity at the base rapidly decreases (UTPF). Continued expansion of the plug and a decrease in near-bed turbulence intensity eventually lead to the formation of a quasi-laminar plug flow riding on a thin shear layer, where minimal turbulence may exist. These results have led to the studies that investigate mudstone layers in various depositional settings in connection with the dynamics of high mud-concentration flows or fluid muds (e.g., Soyinka and Slatt, 2008; Ichaso and Dalrymple, 2009; Ghadeer and Macquaker, 2011; Mackay and Dalrymple, 2011; Plint, 2014; Hovikoski et al., 2016). Most of these studies are concerned with the deposits of fine-grained sediment gravity flows, which undergo a flow transition from turbulent flows through transitional flows to laminar plug flows as they decelerate until they stop. Estuarine fluid muds are, however, affected by both deceleration and acceleration due to tides. Although Mackay and Dalrymple (2011) studied estuarine fluid-mud deposits, it proposed vertical facies changes formed by only decelerating flows. More research is needed to better understand depositional characteristics and processes of fluid muds in tidal environments.

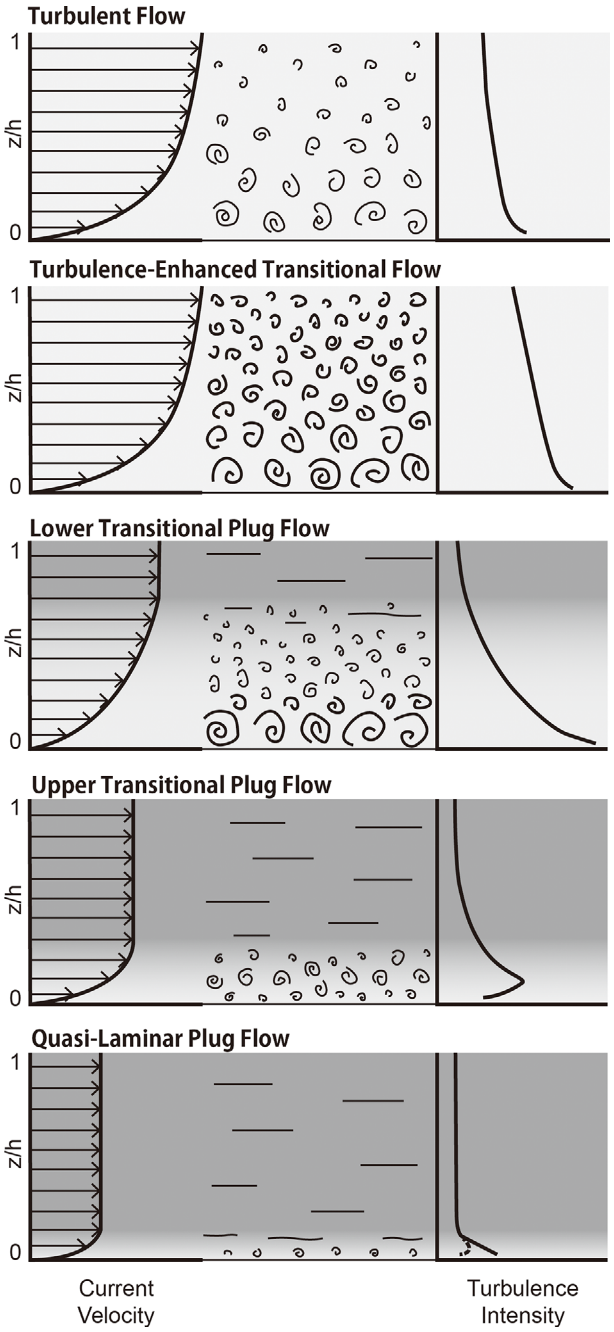

Fig. 1. Schematic model of flow types, which occur as suspended-mud concentration increases. Spirals represent turbulence and horizontal lines indicate laminar flows. Dark-shaded part denotes a cohesive plug. The graphs to the left are characteristic vertical profiles of downstream velocity and those to the right show root-mean-square of downstream velocity, which represents turbulence intensity. The transitional and laminar plug flows occur at the highly-concentrated basal zone of estuarine channel flows. Modified after Baas et al. (2009).

The Early Cretaceous McMurray Formation was formed in the Western Canada foreland basin during a transgression (Leckie and Smith, 1992; Stockmal et al., 1992; Cant, 1996; Hein and Cotterill, 2006). The middle part of the formation was deposited in estuarine environments, mainly consisting of tidally-influenced meandering channel deposits (Mossop and Flach, 1983; Flach, 1984; Flach and Mossop, 1985; Hubbard et al., 2011; Musial et al., 2012; Nardin et al., 2013). Although fluid-mud deposits are likely to occur in the estuarine sequences of the middle McMurray Formation, they have not yet been reported from the formation. In this study, mudstone layers in the middle McMurray Formation are examined in detail through microscopic observations of thin sections of core samples acquired at the Christina Lake area, northeastern Alberta (Fig. 2). One of the main facies of these mudstone layers is structureless mudstone with floating coarse grains within clay matrix, which is a typical characteristics of fluid-mud deposits (Soyinka and Slatt, 2008; Ichaso and Dalrymple, 2009; Ghadeer and Macquaker, 2011; Mackay and Dalrymple, 2011; Plint, 2014). Various subtle structures are also present in the mudstone layers, associated with the structureless mudstone. The aim of this study is to describe in detail the

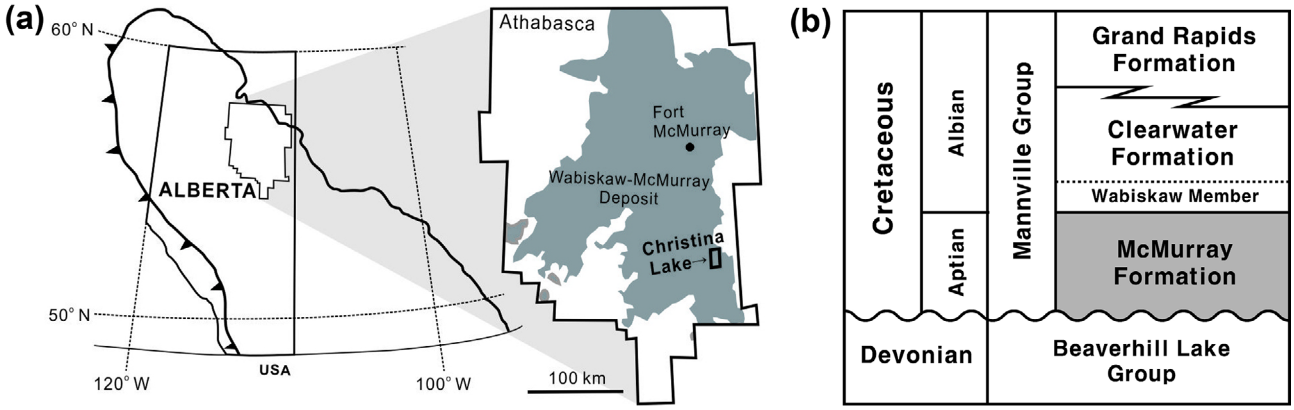

Fig. 2. (a) Location of study area (Christina Lake) in the Western Canada sedimentary basin. Wabiskaw and McMurray oil-sand deposits in the Athabasca area are shaded. Modified from Cant (1996) and Alberta Energy and Utilities Board (2007). (b) Stratigraphy of the Early Cretaceous Manville Group in the study area. The McMurray Formation overlies unconformably the Devonian limestone of the Beaverhill Lake Group.

sedimentary characteristics of these mudstone layers and to interpret their depositional processes based on flow dynamics of fluid muds. Sequences of mudstone layers are also discussed in relation to tidal deceleration and acceleration of fluid muds.

2. STRATIGRAPHY AND DEPOSITIONAL SETTING

The Early Cretaceous McMurray Formation is the lowest formation of the Mannville Group, which was deposited in the Western Canada sedimentary basin during the Aptian to Albian (Fig. 2) (Flach and Mossop, 1985; Leckie and Smith, 1992; Stockmal et al., 1992; Hayes et al., 1994; Cant, 1996; Wightman and Pemberton, 1997; Crerar and Arnott, 2007; Hein, 2015). The McMurray Formation unconformably overlies Devonian carbonates, mainly accumulating in a series of paleovalleys cut into the underlying carbonate rocks (Cant, 1996; Ranger and Pemberton, 1997; Wightman and Pemberton, 1997; Hein and Cotterill, 2006). The formation was deposited during a transgression and is informally divided into three units of lower, middle and upper successions (Mossop and Flach, 1983; Flach, 1984; Flach abd Mossop, 1985; Wightman and Pemberton, 1997; Hein and Cotterill, 2006; Crerar and Arnott, 2007). The lower McMurray succession comprises braided-river deposits that were formed during a sea-level lowstand (Mossop and Flach, 1983; Hein et al., 2000; Hein and Cotterill, 2006; Crerar and Arnott, 2007; Hein, 2015). The middle McMurray succession consists of tidally-influenced channels to estuarine deposits formed in the early stage of transgression (Mossop and Flach, 1983; Flach, 1984; Flach and Mossop, 1985; Hein and Cotterill, 2006; Crerar and Arnott, 2007; Musial et al., 2012). The upper McMurray succession represents bays and marginal marine environments developed in the early to middle stages of transgression (Hein et al., 2000; Hein and Cotterill, 2006; Crerar and Arnott, 2007; Hein, 2015).

The studied core samples (6-5-77-6) were acquired at the Christina Lake area, ca. 140 km south of Fort McMurray, Alberta (Fig. 2a). In this area, the McMurray Formation unconformably overlies the Devonian Beaverhill Lake limestone (Fig. 2b) (Jo and Ha, 2013a; Shinn et al., 2014). The unconformity surface represents the paleotopography, on which the McMurray Formation was deposited, and shows a paleovalley with an ENE-WSW orientation in the southern part (Fig. 3) (Jo and Ha, 2013a, 2013b). The river systems of the McMurray Formation flowed to the east along this paleovalley and merged into the main McMurray river systems that flowed northwards along the Assiniboia valley (Leckie and Smith, 1992; Ranger and Pemberton, 1997; Jo and Ha, 2013a). The thickness of the McMurray formation in the Christina Lake area is 40–130 m, depending on the relief of the sub-Cretaceous unconformity surface; it is thickest along the paleovalley in the southern part. The core is located about 6 km north of the paleovalley (Fig. 3). In the BlackGold Lease area, just west of the Christina Lake area, the distribution of thick channel-sandstone bodies displays channel systems that flowed southwards toward the paleovalley (Fig. 3) (Lee et al., 2015). Such tributary river systems would have developed in the north of the paleovalley in the Christina Lake area, which is also supported by the sedimentary facies described below.

The mudstone beds investigated in this study are present at ca. 20 m above the base of the McMurray Formation (Fig. 4a). The mudstone beds occur within a fining-upward sequence (347.5–341.9 m), in which intraclast breccias and massive sandstones in the lowermost part pass upwards into interbedded sandstones and mudstones (Fig. 4b). The breccias comprise very angular to rounded, granule- to pebble-grade, mudstone clasts and fine- to medium-grained sandstone matrix (Fig. 5a). They show crude stratification, which arises from clast-rich layers and bedding-

https://doi.org/10.1007/s12303-021-0008-4

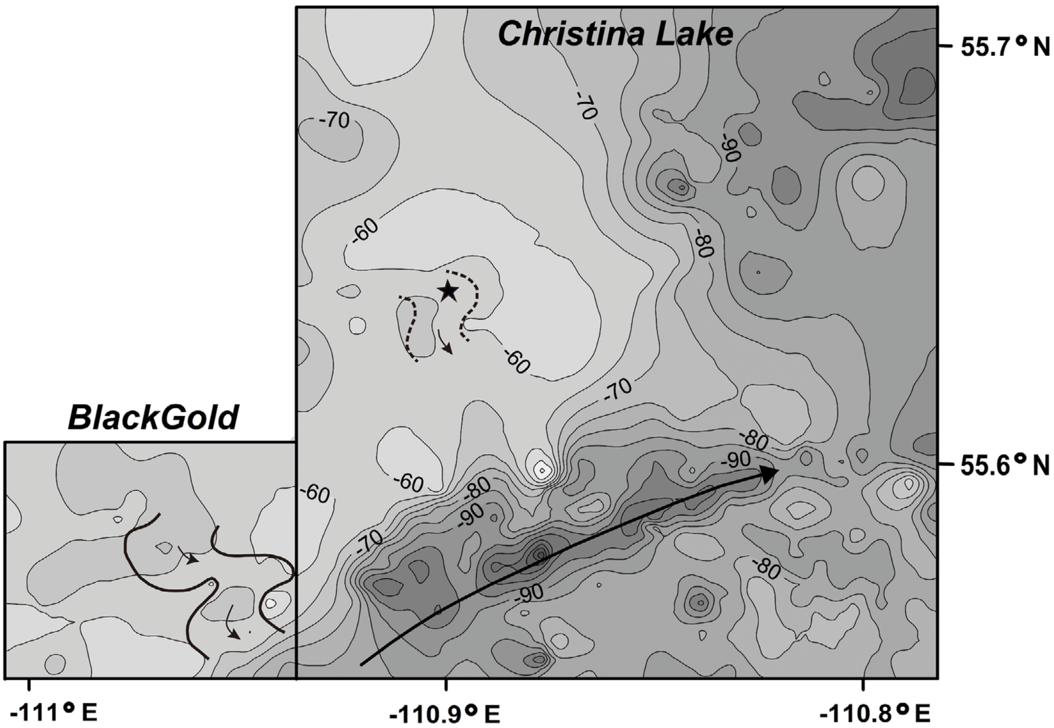

Fig. 3. Paleotopography on the sub-Cretaceous unconformity surface in the Christina Lake and the BlackGold Lease areas. Contours in metres represent the depths of the unconformity surface, measured from the top of the Wabiskaw Member (datum). The location of the studied core is marked with a star. Arrows denote the flow directions of paleo-river systems. Thick solid lines in the BlackGold Lease area show river systems defined by the distribution of thick channel-sandstone bodies at 61 m below the datum. Dashed lines in the Christina Lake area indicate an inferred tributary river system at the core location. Major river systems developed toward ENE along the paleovalley in the southern part.

parallel-oriented mudstone clasts. The intraclast breccias form decimetres-thick beds. The massive sandstones in the lower part are fine- to medium-grained and partly include mudstone intraclasts (Fig. 4b). The massive appearance of some sandstone beds is due to bitumen staining; organic materials show a curvilinear alignment under microscope, possibly tracing stratification (Fig. 5d). In the middle to upper parts of the fining-upward sequence, the interbedded sandstones and mudstones consist of centimetres- to decimetres-thick beds. The sandstones are fine- to medium-grained and either parallel- to cross-laminated or massive (Fig. 4b). The mudstones are either structureless or laminated (Fig. 4b). The interbedded sandstones and mudstones are commonly heterolithic; parallel- and cross-laminated units commonly include alternating sandstone and mudstone laminae (Fig. 5b). In some heterolithic-laminated units, sandstone laminae thin upwards with increasing proportion of interlayered mudstone laminae (Fig. 5c). The dip directions of cross-laminae commonly change vertically to the opposite directions (Fig. 5b). All sandstones forming beds, laminae and matrix of breccias are stained with bitumen.

The fining-upward sequence mainly consisting of interbedded sandstones and mudstones with intraclast breccias and massive sandstones in the lower part is typical deposits of tidally-influenced meandering channels of the McMurray Formation (Mossop and Flach, 1983; Flach and Mossop, 1985; Hubbard et al., 2011; Musial et al., 2011; Nardin et al., 2011). The interbedded sandstones and mudstones represent inclined heterolithic strata formed by lateral migration of point bars (Hubbard et al., 2011; Musial et al., 2011; Nardin et al., 2011). The McMurray deposits showing clearly point-bar morphology in 3-D seismic images mainly consist of heterolithic-stratified sandstones and mudstones (Hubbard et al., 2011). Those heterolithic strata comprise parallel- and cross-laminated sandstones interbedded with laminated and structureless mudstones (Hubbard et al., 2011). The common inclusion of mudstone layers in point-bar strata is indicative of the deposition at the mixing zone of freshwater and seawater; mud deposition is maximized at turbidity maximum zone (La Croix and Dashtgard, 2015; La Croix et al., 2019). The upward thinning of sandstone laminae accompanied with increasing proportion of mudstone laminae in the heterolithic-laminated units most likely resulted from the depositional processes related to spring-neap tidal cycles. Common reversals of the dip directions of cross-laminae are indicative of reversing tidal flows. The intraclast breccias in the lowermost part of the fining-upward sequence are interpreted as resulting from the erosion of cut bank due to lateral migration of meandering channels and the

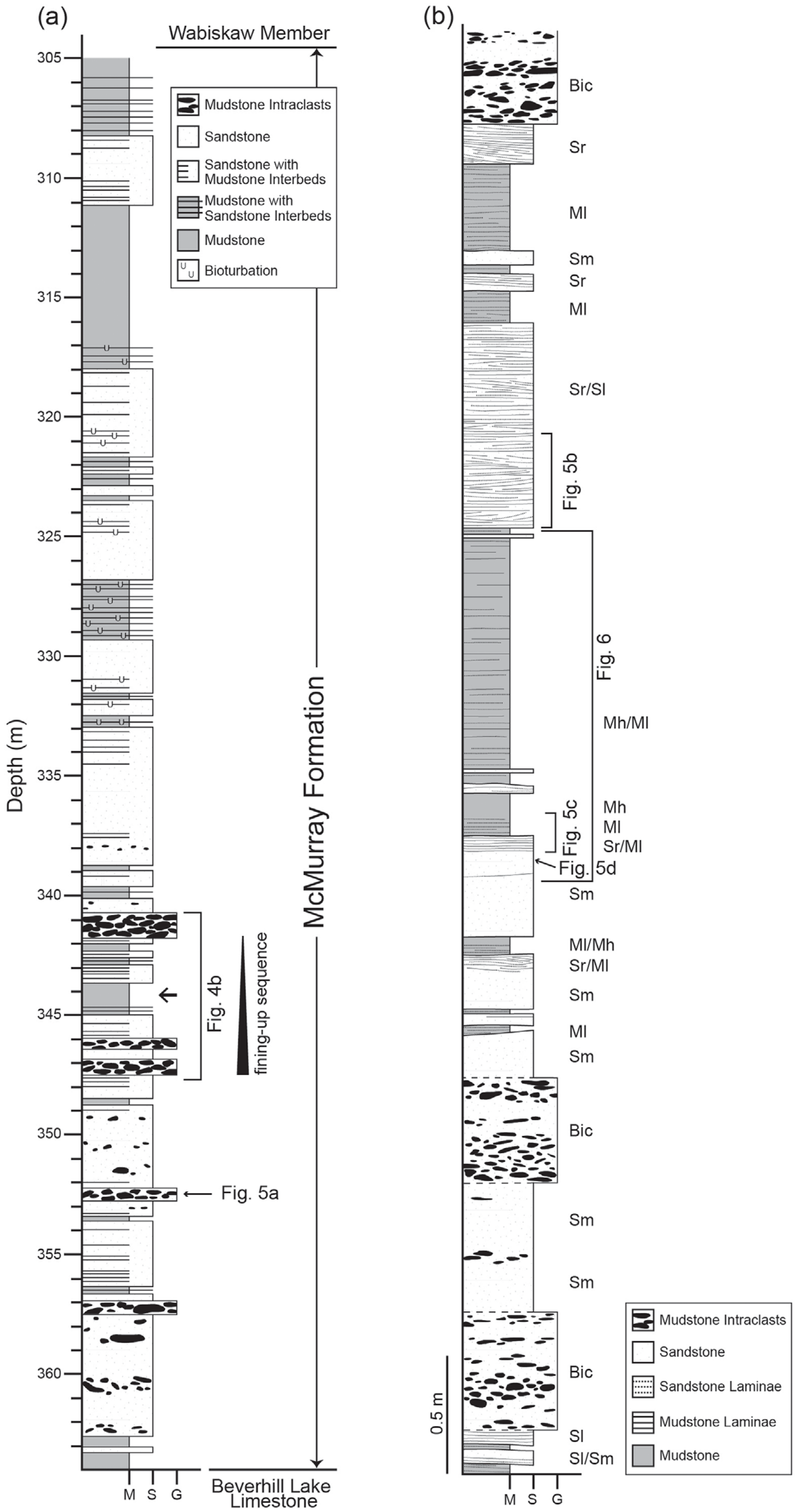

Fig. 4. (a) Columnar log of the McMurray Formation (well 6-5-77-6). A thick arrow indicates the studied mudstone beds, which occur within a fining-upward channel sequence. (b) Columnar log of tidally-influenced channel deposits including the studied mudstone beds. Bic = mudstone-intraclast breccia; Sm = massive sandstone; Sr = cross-laminated sandstone; Sl = parallel-laminated sandstone; Mh = structureless mudstone; Ml = laminated mudstone. Laminations in sandstone and mudstone are commonly heterolithic.

https://doi.org/10.1007/s12303-021-0008-4

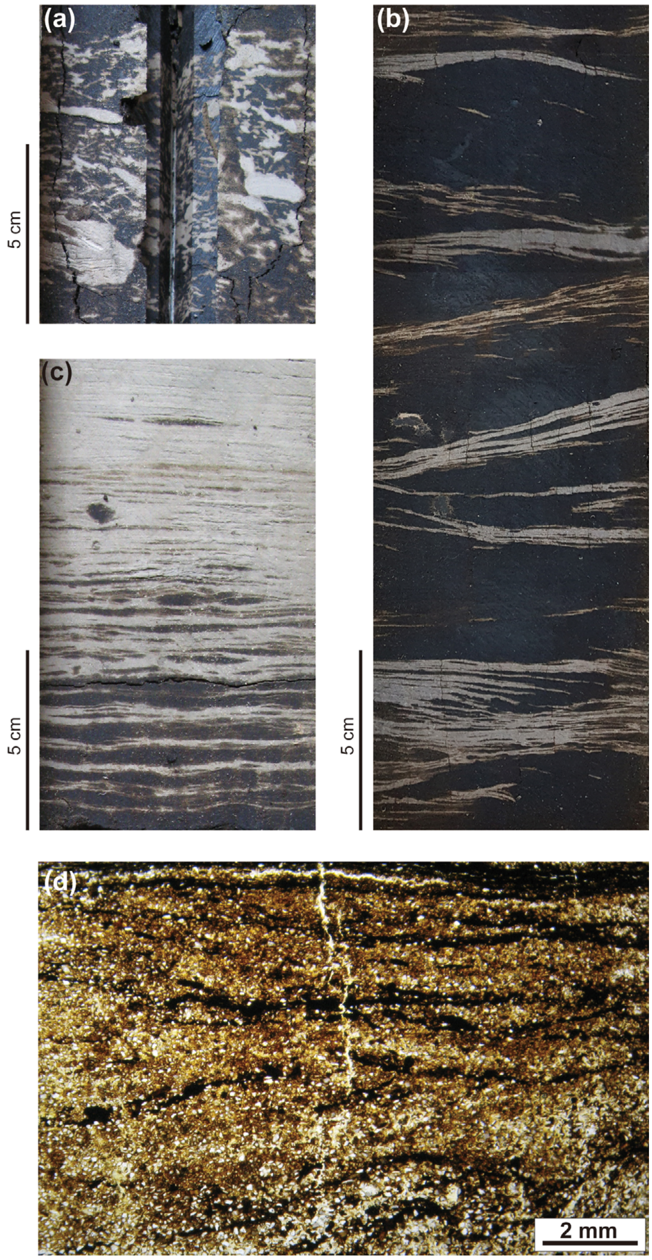

Fig. 5. Photographs of core samples showing typical facies of tidally-influenced channel deposits of the middle McMurray succession. Sandstone is black or dark grey due to bitumen staining. (a) Mudstone-intraclast breccia with bitumen-stained sandstone matrix. (b) Parallel- and cross-laminated sandstones with heterolithic laminations. (c) Heterolithic laminated sandstone and mudstone, in which mudstone laminae increase upwards in proportion accompanied with an upward-thinning of sandstone laminae, probably representing a spring-neap cycle. (d) A micrograph of a massive sandstone bed, showing curvilinear alignments of organic materials (black), suggestive of the presence of stratification. The massive appearance of some sandstone beds is probably due to bitumen staining.

deposition of the eroded bank materials on the channel floor (Hubbard et al., 2011; Musial et al., 2011). Crude stratification and some rounded clasts of the breccias suggest that the mudstone clasts might have been transported as bedload, although they would travel for short distance, and deposited with sandy channel-bed sediment. Such intraclast breccias are common in the basal part of the McMurray channel deposits, overlain by inclined heterolithic strata of point bars (Hubbard et al., 2011; Musial et al., 2011). Overall sedimentary characteristics are suggestive of the deposition in tidally-influenced meandering channels, consistent with the previous depositional models of the McMurray channels (Musial et al., 2011; Nardin et al., 2013).

3. FACIES ANALYSIS OF MUDSTONES

The mudstone beds appear mostly structureless at the hand-specimen scale, sparsely interlayered with faint laminae. A variety of subtle sedimentary structures and layers are, however, recognized through microscopic observations of the thin sections of the mudstones (Fig. 6). Bioturbation is almost absent. To reveal the depositional processes of these mudstone layers, they are classified into three microfacies on the basis of textures and sedimentary structures that can be discerned through microscopic observations: (1) structureless mudstone, (2) silt-streaked mudstone and (3) heterolithic laminated mudstone. These microfacies form layers of less than 1 mm to a few cm in thickness and pass vertically into one another with either transitional or sharp boundaries.

3.1. Microfacies 1 (F1): Structureless Mudstone

3.1.1. Description

This microfacies consists of structureless mudstone that ranges from 1 mm to 25 mm in thickness. Coarse quartz grains of coarse silt to fine sand, occasionally reaching up to medium sand, are dispersed randomly throughout layers (Figs. 7a and b). The matrix is mainly composed of clay particles and shows 'grainy texture' of Plint (2014) (Fig. 7b). Organic materials are abundant with platy particles aligned parallel to bedding. The lower and upper boundaries of Microfacies 1 are transitional with Microfacies 2, but are sharp with Microfacies 3 (Fig. 7c). At the upper boundaries, local depressions are common due to loading by the overlying Microfacies 3 (Fig. 7c).

3.1.2. Interpretation

Structureless mudstone is interpreted as the deposits of cohesive mud flows, i.e., fluid muds, based on the absence of grading, the lack of internal lamination and abundant dispersed coarse grains (Soyinka and Slatt, 2008; Ichaso and Dalrymple, 2009; Mackay and Dalrymple, 2011; Plint, 2014; Hovikoski et al., 2016). As the concentration of clay particles increases, the particles attract one another due to surficial electrostatic forces and form clay flocs (Wang and Larsen, 1994; Baas and Best, 2002; Plint, 2014). The grainy texture of this microfacies indicates the

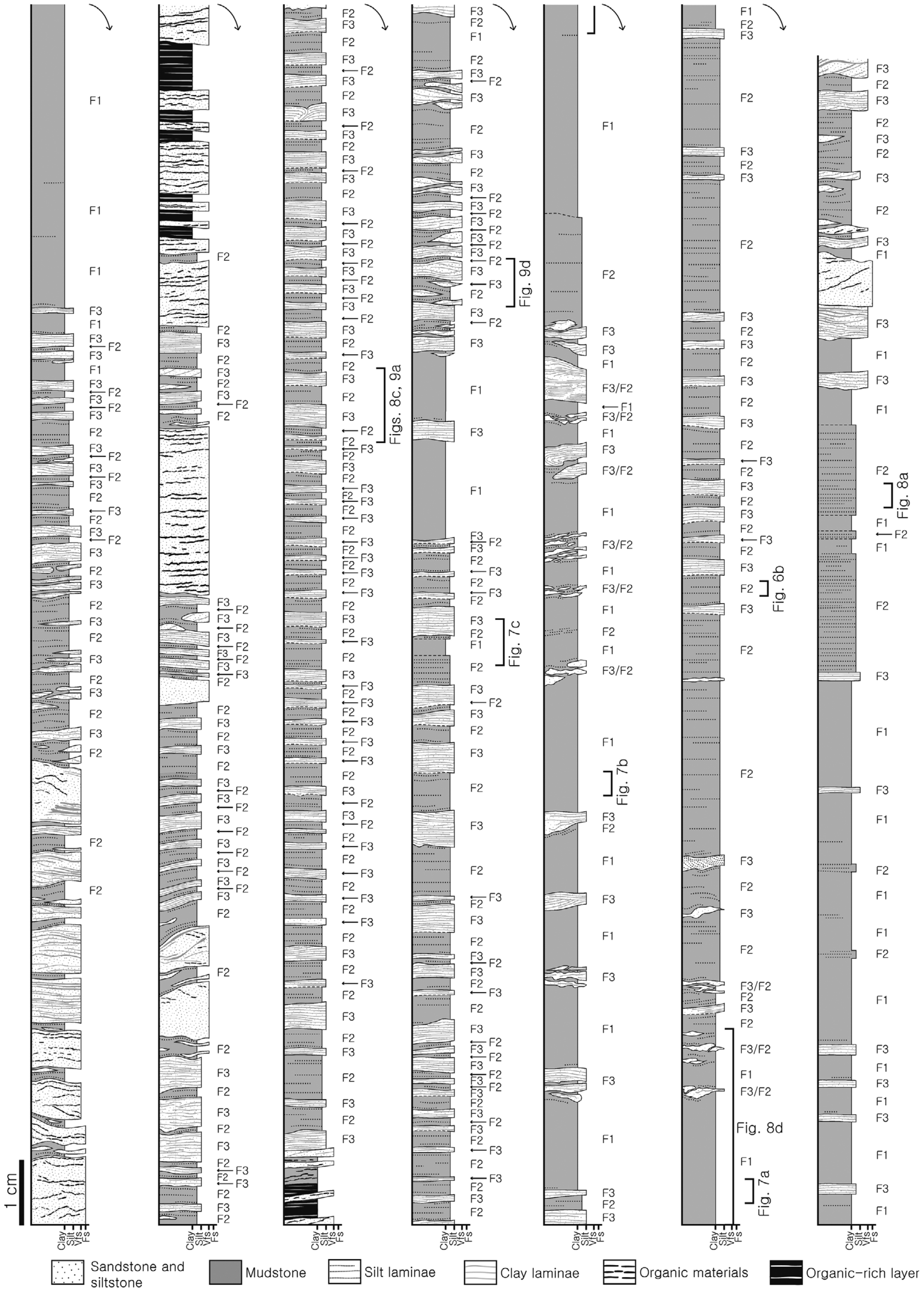

Fig. 6. Detailed columnar logs of mudstone layers, obtained from microscopic observation. Microfacies codes are on the right of columns. F1 = structureless mudstone; F2 = silt-streaked mudstone; F3 = heterolithic laminated mudstone.

https://doi.org/10.1007/s12303-021-0008-4

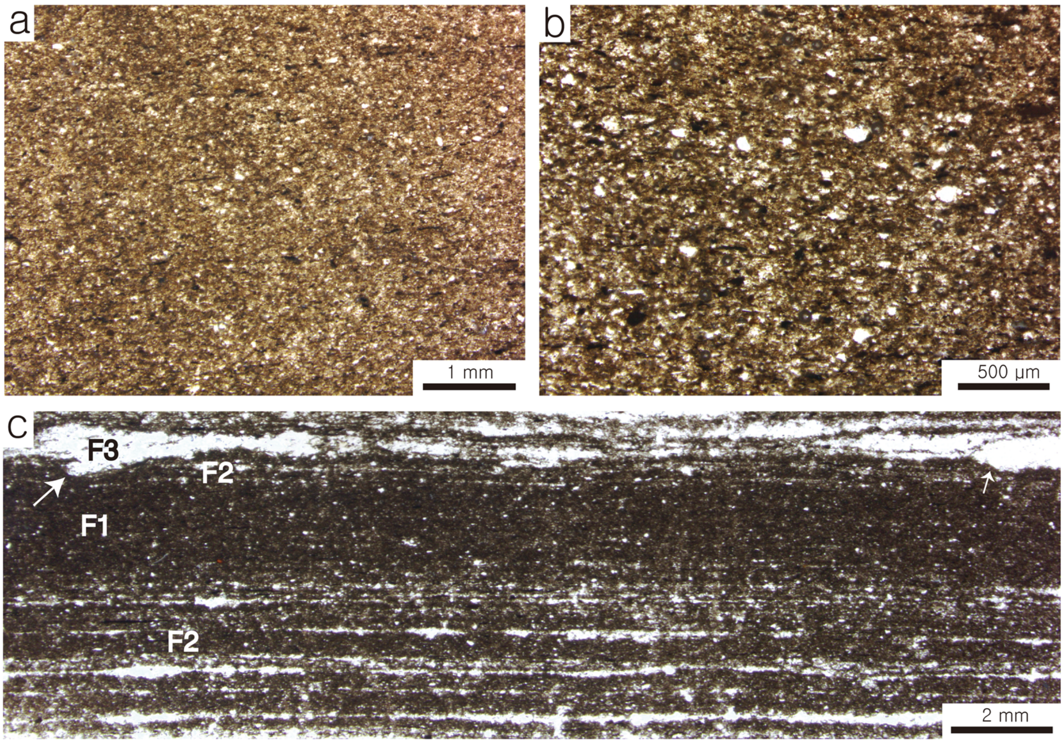

Fig. 7. Micrographs of structureless mudstones (Microfacies 1). (a) Structureless mudstone showing grainy texture and dispersed coarse grains and organic materials (black). (b) Detail view of structureless mudstone, showing grainy texture and dispersed coarse grains and organic materials (black). (c) Microfacies 1 (F1) overlying and underlying Microfacies 2 (F2) with transitional boundaries. Load structure (large arrow) and small erosional structure (small arrow) are present at the base of the overlying Microfacies 3 (F3).

presence of clay flocs or aggregates in highly-concentrated mud suspension (Plint, 2014). The clay particles in clay flocs show a random orientation rather than a preferred bedding-parallel orientation, which together with silt grains included in the flocs gives rise to grainy texture (Plint, 2014). The cohesive clay particles and flocs can suppress most turbulence throughout the high-concentration layer, forming a plug (Baas and Best, 2002; Bass et al., 2009, 2011). In the plug, there are sufficient cohesive forces to support suspended coarse grains, resulting in dispersed coarse grains throughout the mud layer (Baas and Best, 2002; Ichaso and Dalymple, 2009; Plint, 2014). The fluid muds forming Microfacies 1 are thought to be quasi-laminar plug flows because of the textures indicative of cohesive strength and little evidence for flow turbulence. It is estimated that the thickness of the fluid-mud layers before compaction was greater than 1 cm and reached a few decimetres, based on about 90% or more porosities of the recent fluid-mud deposits (Traykoski et al., 2000).

3.2. Microfacies 2 (F2): Silt-streaked Mudstone

3.2.1. Description

This microfacies comprises mudstone with very thin, discontinuous silt streaks or laminae (Fig. 8). The facies units are usually 2 to 10 mm thick, but occasionally form stacked layers reaching up to 28 mm in thickness. This mudstone is similar to Microfacies 1 in texture, containing dispersed coarse quartz grains of medium silt to very fine sand and organic particles (Fig. 8b). Grainy texture and absence of grading are also characteristic of this microfacies. The silt streaks are sub-millimetres thick and consist of coarse-silt to very-fine-sand grains. They are parallel to the layers and normally discontinuous. They tend to extend longer at the transitions to Microfacies 3 (Fig. 8c). The boundaries with the overlying Microfacies 3 are generally gradational, but commonly sharp with the underlying Microfacies 3 (Fig. 8c). This microfacies is also vertically associated with Microfacies 1 with gradational boundaries (Fig. 7c). Microfacies 2 interlayered with relatively thick Microfacies 1 is commonly deformed (Fig. 8d).

3.2.2. Interpretation

Silt-streaked mudstone is also interpreted as being deposited from fluid muds. The scarcity of grading, randomly dispersed coarse grains and grainy texture indicate that this microfacies was deposited by cohesive mud flows with clay flocs (Plint, 2014; Hovikoski et al., 2016). The silt streaks are, however, suggestive of the presence of intermittent turbulence, which segregated coarse-silt to very-fine-sand grains from cohesive mud suspension (Baas and Best, 2002). In upper transitional plug flows or quasi-

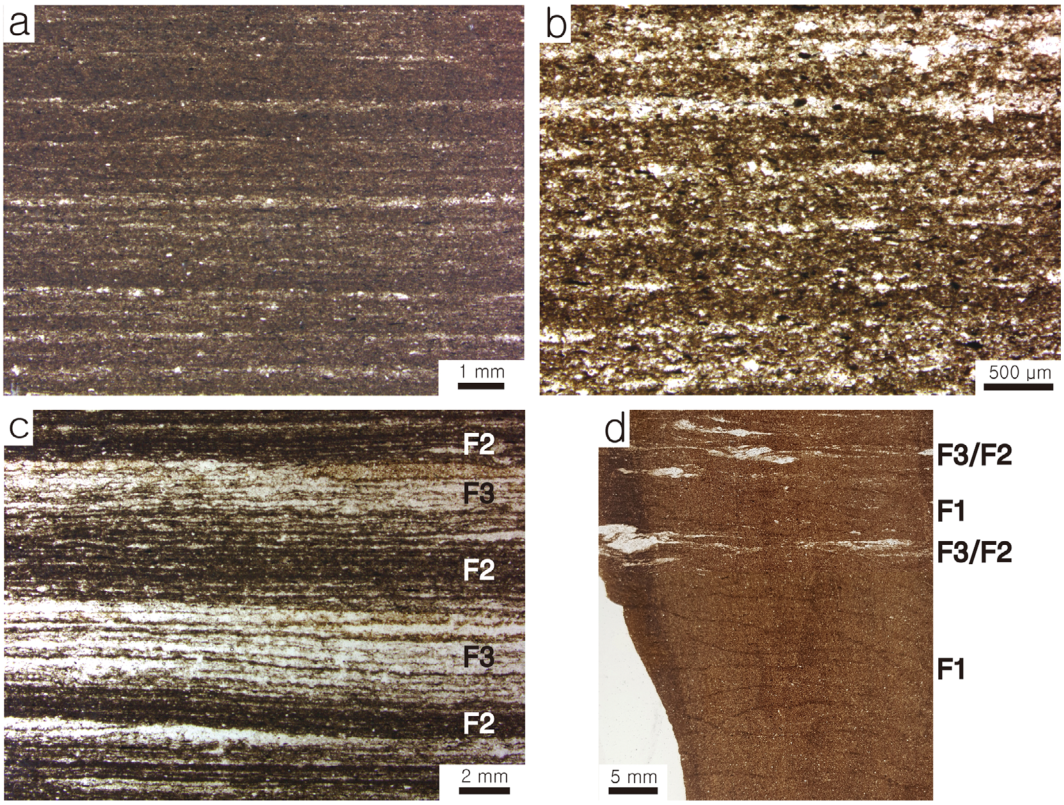

Fig. 8. Micrographs of silt-streaked mudstone (Microfacies 2). (a) Very thin, streaks of coarse-silt to very-fine-sand grains in Microfacies 2. (b) Detail view showing the texture of silt-streaked mudstone: grainy texture and dispersed coarse grains and organic particles (black). (c) Alternations of microfacies 2 (F2) and 3 (F3) with either transitional or sharp boundaries. (d) Deformed microfacies 2 (F2) and 3 (F3) associated with relatively thick Microfacies 1 (F1).

laminar plug flows with relatively low concentrations, turbulence induced by shear at the bed is dampened by cohesive forces, but not fully suppressed, resulting in residual turbulence near the bed (Baas and Best, 2002; Baas et al., 2009, 2011). The segregated silt grains were most likely transported as bedload, forming silt streaks. The bedload grains would move for short distance due to high settling rates of clay flocs in the upper transitional plug flows (Baas et al., 2016). Deformation of this microfacies is ascribed to high water content of the associated thick Microfacies 1.

3.3. Microfacies 3 (F3): Heterolithic Laminated Mudstone

3.3.1. Description

Heterolithic laminated mudstone is composed of alternating, very thin, silt and clay laminae, which form lamina-sets of < 1 to 4 mm in thickness (Fig. 9). The silt laminae consist of coarse-silt to very-fine-sand grains and are usually much thicker than clay laminae. The lamina-sets are characterized by either parallel to sub-parallel lamination or low-angle cross-lamination (Figs. 9b and c). Some layers consist of a few vertically stacked lamina-sets, which are discerned by subtle changes in lamina attitude (Fig. 9c). Some low-angle cross-laminated sets are lenticular, surrounded by Microfacies 2 layers, or show low-amplitude ripple forms with sigmoidal heterolithic cross-lamination (Fig. 9d). This microfacies is commonly bounded by sharp, gently-scoured, upper boundaries (Figs. 9b and c). Low-angle cross-laminae are commonly present below and/or laterally associated with the scour surfaces, forming the uppermost part of the layers (Figs. 9b and c). The lower boundaries are also sharp, but occasionally transitional with the underlying Microfacies 2 layers (Fig. 9a). Load structures and small-scale (< 5 mm wide) erosional structures with concave-up geometry are common at the lower boundaries (Figs. 7c and 9d). Microfacies 3 interlayered with relatively thick Microfacies 1 is commonly deformed (Fig. 8d).

3.3.2. Interpretation

The heterolithic laminae associated with cohesive mud-flow deposits (Microfacies 1 and 2) are interpreted as the products of shear sorting under the cohesive plugs (Mackay and Dalrymple, 2011; Plint, 2014; Hovikoski et al., 2016). As suspended mud concentrations increase, turbulent flows are transformed into transitional plug flows, which have an upper cohesive plug and a lower turbulent zone (Baas and Best, 2002; Baas et al., 2009, 2011).

 https://doi.org/10.1007/s12303-021-0008-4

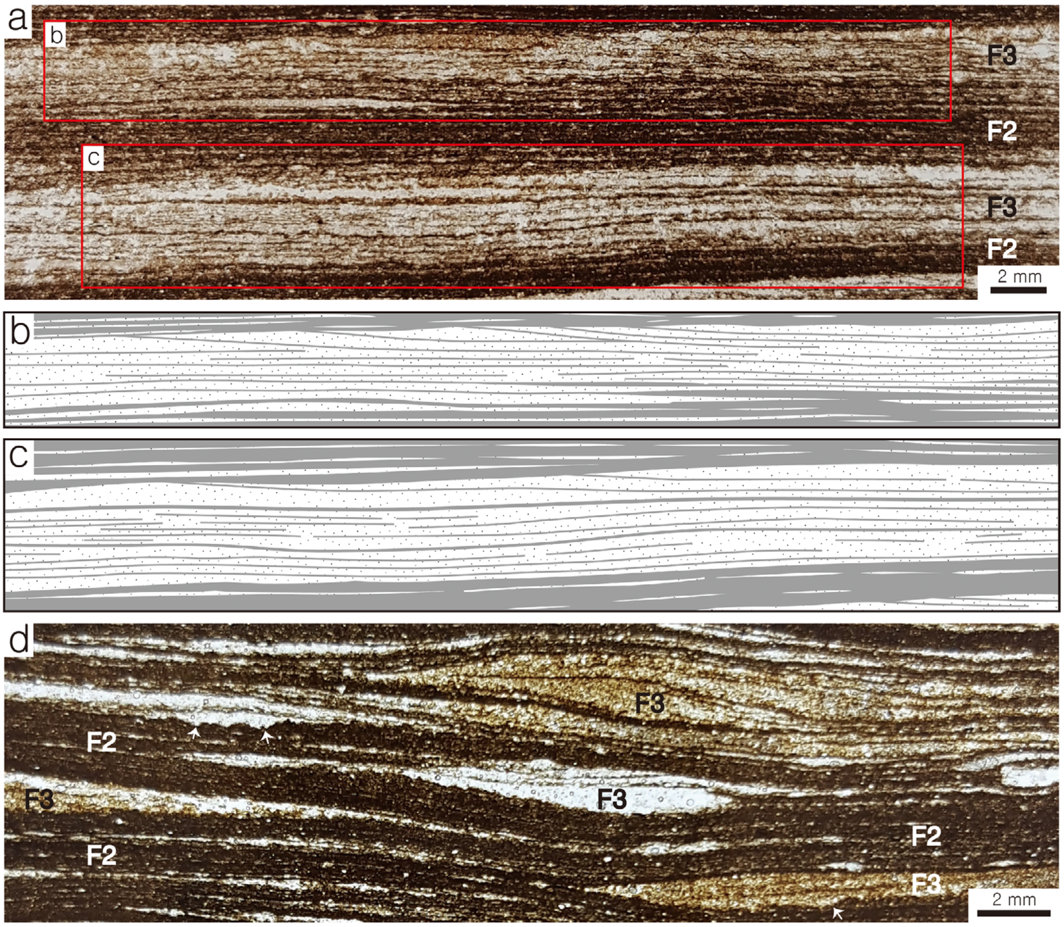

Fig. 9. Micrographs and sketches of heterolithic laminated mudstone (Microfacies 3). (a) Two layers of Microfacies 3 (F3) consisting of alternating silt and clay laminae. Silt laminae are much thicker than clay laminae. The laminae are either parallel to subparallel or low-angle cross-laminated. (b) A sketch of the upper layer in Figure 9a, showing parallel lamination in the lower part and low-angle cross-lamination in the uppermost part. Note a gentle scour surface at the top of the layer. (c) A sketch of the lower layer in Figure 9a. This layer of Microfacies 3 comprises three lamina-sets, which are discerned by subtle differences in lamina attitude and bounded by relatively continuous and distinct clay laminae. The laminae in the lower two sets are parallel to subparallel. The uppermost set is low-angle cross-laminated, gently scoured at the top. (d) Lenticular sets of Microfacies 3 (F3), showing low-angle cross-lamination and low-amplitude ripple forms. Tiny erosional structures (arrows) are present at the base of some layers.

Within the turbulent zone, velocity fluctuations are generated by Kelvin-Helmholtz instabilities at the boundary between the two zones. These velocity fluctuations can result in the alternating deposition of silt and clay grains (Bass and Best, 2002; Mackay and Dalrymple, 2011).

The heterolithic laminae of this microfacies are similar to those of low-amplitude bed-waves or ripples produced under lower transitional plug flows (Baas et al., 2011, 2016). The bedforms responsible for parallel to sub-parallel laminations would be nearly flat or have a gentle relief. The dominantly vertical stacking of these laminae suggests that the bedforms mainly aggraded vertically. Low-angle cross-lamination is also commonly formed under such transitional flows (Mackay and Dalrymple, 2011; Baas et al., 2016).

The change from vertically stacked laminae to low-angle cross-laminae in the uppermost part and scoured top surfaces can be attributed to increasing intensities of near-bed turbulence with increasing clay concentrations in lower transitional plug flows (LTPFs) (Baas et al., 2009, 2011, 2016). In LTPFs with relatively low concentrations, vertical aggradation of bedforms would be dominant due to relatively high rates of suspension settling (Baas et al., 2016). As suspended sediment concentrations increase, near-bed turbulence becomes stronger and reaches highest intensity just before the transition to upper transitional plug flows (Baas et al., 2009, 2011). The strong turbulence would inhibit settling of suspended sediments, especially of clay particles, and erode and rework bed materials (Baas et al., 2011, 2016). The clay flocs on the bed might have been broken and resuspended by strong turbulence. The eroded silt grains were probably transported downstream to form low-amplitude bed-waves, producing silt-dominant, low-angle cross-lamination. Lateral migration of the bed-waves was dominant over vertical aggradation due to low rates of suspension settling and active reworking of bed sediments. The scoured surfaces would expand downstream with time and eventually begin to erode the associated bed-waves downstream, resulting in gentle erosional surfaces on the uppermost low-angle cross-laminae. The scours at the top of this microfacies and the associated low-angle cross-laminae thus indicate that bed sediments were eroded by strong turbulence and redeposited downstream as low-amplitude bed-waves in lower transitional plug flows. The loading and deformation structures can be attributed to high water content of the associated Microfacies 1 and 2 layers.

Bedload deposition of silt and mud floccules is one of possible depositional processes of heterolithic laminated mudstone and silt-laminated mudstone (Yawar and Schieber, 2017). The flows of their experiments appear turbulent and more dilute than those of Baas et al. (2011, 2016), although the flow characteristics of the basal highly-concentrated layer is not clearly defined. Both silt and floccule ripples migrate over the same surface and leave behind thin veneers of sediments, resulting in mud beds containing discontinuous silt laminae (Yawar and Schieber, 2017). This depositional process is likely to produce randomly-distributed silt laminae within mud layers rather than alternation of silt and clay-rich laminae. The heterolithic cross-laminated layer is similar to internally heterolithic-laminated ripples formed by transitional flows of Bass et al. (2011, 2016). The ripples produced by Yawar and Schieber (2017) do not comprise internal heterolithic laminae. Deposition of silt and floccule ripples as thin veneers of sediments is likely to occur at low sedimentation-rate conditions (Yawar and Schieber, 2017). The mudstone layers of this study are, however, thought to be deposited in relatively high sedimentation-rate conditions because of common load structures and soft sediment deformation indicating high water content of rapidly deposited mud. The absence of bioturbation is also indicative of rapid deposition of mud, otherwise it would be common in tidal muds (Mackay and Dalrymple, 2011). Deposition from transitional plug flows is compatible with the characteristics of heterolithic laminated mudstone (Microfacies 3).

4. DISCUSSION: TIDALLY-INFLUENCED DEPOSITION OF FLUID MUDS

The experimental studies of high clay-concentration flows clearly show that clay content controls the relative intensity of two compelling forces (turbulent vs. cohesive) within the flows, resulting in various flow types (Baas and Best, 2002; Baas et al., 2009, 2011, 2016). The results of these experiments have been applied to the deposits of decelerating, fine-grained, sediment gravity flows or fluid muds, which are expected to change their flow types with deceleration (e.g., Ghadeer and Macquaker, 2011; Plint, 2014; Hovikoski et al., 2016). In tidally-influenced environments, fluid muds are most likely to experience both deceleration and acceleration with tidal cycles. Although Mackay and Dalrymple (2011) suggested only fining-upward facies sequences formed by decelerating fluid muds toward a slack water, sequences by accelerating flows can also form in such environments. The vertical changes of microfacies revealed in this study suggest that the deposition by fluid muds occurred with both increasing and decreasing suspended sediment concentrations (SSCs) and thus with deceleration and acceleration of flows. Based on the vertical changes of microfacies and the recent understanding of flow dynamics of high mud-concentration flows, an ideal microfacies sequence and depositional processes of tidally-influenced fluid muds are proposed. The vertical changes can be grouped into two types of microfacies sequences: increasing-SSC and decreasing-SSC sequences (Fig. 10). A number of alternations of these sequences are most probably due to tidal influence (Fig. 6).

The increasing-SSC sequence is formed as fluid muds decelerate and near-bed SSCs increase. Flow types thus change from a lower transitional plug flow (LTPF) through an upper transitional plug flow (UTPF) to a quasi-laminar plug flow (QLPF). The sequence consisting of heterolithic laminated mudstone (Microfacies 3), silt-streaked mudstone (Microfacies 2) and structureless mudstone (Microfacies 1) in ascending order represents this flow transition (Fig. 10). In LTPFs with relatively strong near-bed turbulence, coarse grains (silt to fine sand) move as bedload along with settling of clay flocs, forming low-amplitude bed-waves (Baas et al., 2016). Parallel-lamination or low-angle cross-lamination comprising heterolithic laminae is produced (Microfacies 3). As LTPFs slow down and near-bed SSCs increase, the intensity of near-bed turbulence increases and reaches a peak magnitude just before the flows change to UTPFs (Baas et al., 2009, 2011, 2016). The increased turbulence intensities may hamper settling of clay flocs and cause destruction of clay flocs, resulting in dominance of coarse grains on the bed. The coarsening-upward trend with increasing proportion and thickness of silt laminae in some heterolithic laminated layers (Microfacies 3) represents the increasing turbulence intensities with deceleration of LTPFs (Figs. 8c and 9a). At the maximum turbulence intensity of LTPFs, bed materials are eroded and reworked, producing scoured surfaces (Baas et al., 2011, 2016). Resuspended clay particles would not be able to settle down due to strong turbulence. Eroded silt grains are transported as bedload, forming low-amplitude bed-waves downstream of the scour (Baas et al., 2016). The scoured surface and the associated bed-waves migrate downstream with little vertical aggradation. The top of heterolithic laminated mudstone (Microfacies 3) is thus commonly characterized by sharp scoured surfaces and low-angle cross-laminated silt laminae

 https://doi.org/10.1007/s12303-021-0008-4

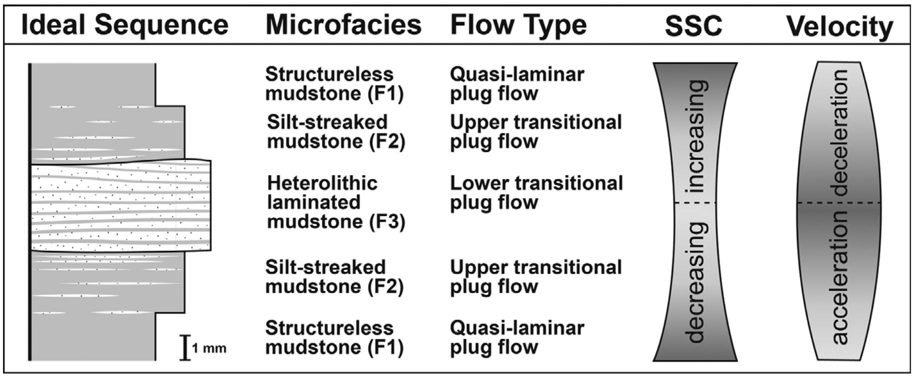

Fig. 10. Ideal sequence of tidally-influenced fluid muds. Flow types change from quasi-laminar plug flows (QLPF) through upper transitional plug flows (UTPF) to lower transitional plug flows (LTPF) as the flow accelerates and suspended sediment concentration (SSC) decreases, resulting in the deposition of structureless mudstone (F1), silt-streaked mudstone (F2) and heterolithic laminated mudstone (F3) in ascending order. During a flow deceleration and a resultant increasing SSC, a reversed microfacies sequence is formed by a reversed change in flow types.

(Figs. 9b and c). Given enough time, the scour would become deeper and the bed-waves would grow into ripples larger than those in turbulent flows (Baas et al., 2011, 2016). Deep scours and large ripples, however, are not likely to develop under estuarine fluid muds, because of high aggradation rates and rapid changes in flow types.

With a further decrease in flow velocity and an increase in SSC, the flow transforms into an UTPF, where the cohesive plug becomes thicker and the near-bed turbulence weakens greatly (Baas and Best, 2002; Baas et al., 2009). Cohesive force increases rapidly so that it could support silt grains (Baas et al., 2011, 2016). Mixed clay and silt sediments are deposited. The near-bed turbulence, although it is much weaker than that of LTPFs, could segregate some silt grains from clay particles. The silt grains would be transported as bedload, but in a short duration and short distance, because they are quickly buried by the rain of suspended sediments. Streaks and discontinuous laminae of silt grains are preserved in the mixed silt and clay sediments (Microfacies 2). As the flow slows down further, it changes to a QLPF, where the cohesive plug expands to the bed and the near-bed turbulence almost disappears (Baas and Best, 2002; Baas et al., 2009). Coarse grains of silt to fine sand are supported by cohesive forces within the plug (Sumner et al., 2009; Baas et al., 2011, 2016). The freezing of the QLPF produces structureless mudstone with dispersed coarse grains (Microfacies 1).

A decreasing-SSC sequence represents the deposition of fluid muds during acceleration by tidal influence (Fig. 10). Overlying flows exert shear stresses increasingly on the fluid mud, stirring the whole or the upper part of the previously-deposited fluid-mud layer and reducing the cohesive forces within the layer. The layer with reduced cohesive strengths could move, driven by the overlying flows. Or, if the upper part of the fluid mud is mobile, it could easily move by the accelerating, overlying flows (Kirby and Parker, 1983). In these ways, the fluid-mud layer on the bottom begins to flow again. As the overlying flows accelerate, the stirring action from the top of the fluid mud becomes stronger and the cohesive forces within the fluid mud decrease, resulting in a transformation into an UTPF. Silt-streaked mudstone (Microfacies 2) is deposited by UTPFs on the previous structureless mudstone (Microfacies 1) of QLPFs. Continued acceleration, stirring and mixing with the overlying turbulent flows further reduce the cohesive forces of the fluid mud. The UTPF eventually transforms into a LTPF. Under LTPFs, parallel-laminated or low-angle cross-laminated heterolithic layers (Microfacies 3) are deposited on the silt-streaked mudstone (Microfacies 2) of UTPFs. At the transition from Microfacies 2 to 3, the maximum turbulence intensity of LTPFs is recorded as tiny erosional structures at the base of Microfacies 3 (Figs. 7c and 9d), unlike the relatively broad scour surfaces at the transition from Microfacies 3 to 2. This is probably due to high cohesive strength of the clay-rich sediment deposited by the previous UTPFs.

The sequences described above are ideal sequences that can be formed during tidal acceleration and deceleration of fluid muds. Parts of the sequences may be missing, depending on suspended sediment concentrations. In the periods of high suspended-mud concentrations, sequences consisting of structureless mudstone and silt-streaked mudstone may be deposited by QLPFs and UTPFs. At relatively low concentrations, the sequences may comprise only silt-streaked and heterolithic laminated mudstones deposited by UTPFs and LTPFs. If fluid muds are significantly diluted and transformed into turbulent flows, clean sand layers might be deposited in association with fluid-mud layers (e.g., Mackay and Darlymple, 2011; Plint, 2014). Parts of the sequences can also not be deposited due to short durations of particular flow types. The proposed depositional model of tidally-influenced fluid muds needs further verification through more studies on other estuarine sequences.

5. CONCLUSIONS

Tidally-influenced channel deposits in the middle McMurray Formation (Early Cretaceous) at the Christina Lake area, Alberta, Canada include mudstone beds of high mud-concentration flows, i.e., fluid muds. These mudstone beds comprise numerous thin layers (< 1–25 mm thick), which are classified into three microfacies on the basis of microscopic textures and structures and represent a range of flow types of fluid muds. Structureless mudstone (Microfacies 1) containing dispersed coarse grains is indicative of the deposition by cohesive mud flows with sufficient cohesive forces to support coarse grains (quasi-laminar plug flow). Silt-streaked mudstone (Microfacies 2) is also interpreted as the deposits of cohesive fluid muds, but with weak turbulence under the cohesive plug (upper transitional plug flow). Heterolithic laminated mudstone (Microfacies 3) consisting of alternating silt and clay laminae would be deposited by low-amplitude bed-waves formed in lower transitional plug flows that have a relatively strong turbulence beneath a cohesive plug. As a result of tidal deceleration and acceleration, the deposition by fluid muds appears to have occurred with increasing and decreasing suspended mud concentrations and with resultant changes in flow types. An ideal sequence of tidally-influenced fluid muds is proposed. During deceleration and increasing mud concentrations, Microfacies 3, 2 and 1 are deposited in ascending order as flow types change from lower transitional plug flows through upper transitional plug flows to quasi-laminar plug flows. During acceleration and decreasing mud concentrations, the three microfacies are deposited in the reversed order with the reversed changes in flow types. Parts of the sequences may not be deposited, depending on suspended sediment concentrations and the durations of particular flow types.

ACKNOWLEDGMENTS

This research was supported by Basic Science Research Program through the National Research Foundation of Korea (NRF) funded by the Ministry of Education (2017R1D1A1B03034796).

REFERENCES

Alberta Energy and Utilities Board, 2007, Alberta's Energy Reserves 2006 and Supply/Demand Outlook 2007–2016. AEUB ST98-2007, Calgary, 218 p.

Baas, J.H. and Best, J.L., 2002, Turbulence modulation in clay-rich sediment-laden flows and some implications for sediment deposition. Journal of Sedimentary Research, 72, 336–340.

Baas, J.H., Best, J.L., and Peakall, J., 2011, Depositional processes, bedform development and hybrid bed formation in rapidly decelerated cohesive (mud-sand) sediment flows. Sedimentology, 58, 1953–1987.

Baas, J.H., Best, J.L., and Peakall, J., 2016, Predicting bedforms and primary current stratification in cohesive mixtures of mud and sand. Journal of the Geological Society, 173, 12–45.

Baas, J.H., Best, J.L., Peakall, J., and Wang, M., 2009, A phase diagram for turbulent, transitional, and laminar clay suspension flows. Journal of Sedimentary Research, 79, 162–183.

Cant, D.J., 1996, Sedimentological and sequence stratigraphic organization of a foreland clastic wedge, Mannville Group, Western Canada Basin. Journal of Sedimentary Research, 66, 1137–1147. https://doi.org/10.1306/D42684C3-2B26-11D7-8648000102C1865D

Crerar, E.E. and Arnott, R.W.C., 2007, Facies distribution and stratigraphic architecture of the Lower Cretaceous McMurray Formation, Lewis Property, northeastern Alberta. Bulletin of Canadian Petroleum Geology, 55, 99–124.

Dalrymple, R.W. and Choi, K.S., 2007, Morphologic and facies trends through the fluvial-marine transition in tide-dominated depositional systems: a schematic framework for environmental and sequence-stratigraphic interpretation. Earth-Science Reviews, 81, 135–174.

Flach, P.D., 1984, Oil Sands Geology—Athabasca deposit north. Alberta Research Council, Edmonton, 31 p.

Flach, P.D. and Mossop, G.D., 1985, Depositional environments of Lower Cretaceous McMurray Formation, Athabasca oil sands, Alberta. American Association of Petroleum Geologists Bulletin, 69, 1195–1207. https://doi.org/10.1306/AD462BAF-16F7-11D7-8645000102C1865D

Ghadeer, S.G. and Macquaker, J.H.S., 2011, Sediment transport processes in an ancient mud-dominated succession: a comparison of processes operating in marine offshore settings and anoxic basinal environments. Journal of the Geological Society, 168, 1121–1132.

Hayes, B.J.R., Christopher, J.E., Rosenthal, L., Los, G., McKercher, B., Minken, D., Tremblay, Y.M., and Fennell, J., 1994, Cretaceous Mannville Group of the Western Canada sedimentary basin. In: Mossop, G.D. and Shetsen, I. (eds.), Geological Atlas of the Western Canada Sedimentary Basin. Canadian Society of Petroleum Geologists and Alberta Research Council, Special Report, 4, p. 317–334.

Hein, F.J., 2015, The Cretaceous McMurray oil sands, Alberta, Canada: a world-class, tidally influenced fluvial-estuarine system—an Alberta government perspective. In: Ashworth, P.J., Best, J.L., and Parsons, D.R. (eds.), Fluvial-Tidal Sedimentology. Developments in Sedimentology, 68, p. 561–621. https://doi.org/10.1016/B978-0-444-63529-7.00018-3

Hein, F.J. and Cotterill, D.K., 2006, The Athabasca oil sands—a regional geological perspective, Fort McMurray area, Alberta, Canada. Natural Resources Research, 15, 85–102.

Hein, F.J., Cotterill, D.K., and Berhane, H., 2000, An atlas of lithofacies of the McMurray Formation, Athabasca oil sands deposit, northeastern Alberta: surface and subsurface. Earth Sciences Report 2000-07, Alberta Energy and Utilities Board/Alberta Geological Survey, Edmonton, 217 p.

Hovikoski, J., Therkelsen, J., Nielsen, L.H., Bojesen-Koefoed, J.A., Nytoft, H.P., Petersen, H.I., Abatzis, I., Tuan, H.A., Phuong, B.T.N., Dao, C.V., and Fyhn, M.B.W., 2016, Density-flow deposition in a fresh-water lacustrine rift basin, Paleogene Bach Long Vi Graben, Vietnam. Journal of Sedimentary Research, 86, 982–1007.

Hubbard, S.M., Smith, D.G., Nielsen, H., Leckie, D.A., Fustic, M., Spencer, R.J., and Bloom, L., 2011, Seismic geomorphology and sedimentology of a tidally influenced river deposit, Lower Cretaceous Athabasca oil sands, Alberta, Canada. American Association of Petroleum Geologists Bulletin, 95, 1123–1145.

Ichaso, A.A. and Dalrymple, R.W., 2009, Tide- and wave-generated fluid mud deposits in the Tilje Formation (Jurassic), offshore Norway. Geology, 37, 539–542.

Jo, H.R. and Ha, C.G., 2013a, Stratigraphic architecture of fluvial deposits of the Cretaceous McMurray Formation, Athabasca oil sands, Alberta, Canada. Geosciences Journal, 17, 417–427.

Jo, H.R. and Ha, C.G., 2013b, Basal water-bearing zone of the oil-sands deposits of the Cretaceous McMurray Formation at Christina Lake, Alberta, Canada. Geosciences Journal, 17, 445–453.

Kirby, R. and Parker, W.R., 1983, Distribution and behavior of fine sediment in the Severn Estuary and inner Bristol Channel, U.K. Canadian Journal of Fisheries and Aquatic Sciences, 40, 83–95.

La Croix, A.D. and Dashtgard, S.E., 2015, A synthesis of depositional trends in intertidal and upper subtidal sediments across the tidal-fluvial transition in the Fraser River, Canada. Journal of Sedimentary Research, 85, 682–698.

La Croix, A.D., Dashtgard, S.E. and MacEachern, J.A., 2019, Using a modern analogue to interpret depositional position in ancient fluvial-tidal channels: example from the McMurray Formation, Canada. Geoscience Frontiers, 10, 2219–2238.

Leckie, D.A. and Smith, D.G., 1992, Regional setting, evolution, and depositional cycles of the Western Canada foreland basin. In: Macqueen, R.W. and Leckiem D.A. (eds.), Foreland Basins and Fold Belts. American Association of Petroleum Geologists Memoir, 55, p. 9–46.

Mackay, D.A. and Dalrymple, R.W., 2011, Dynamic mud deposition in a tidal environment: the record of fluid-mud deposition in the Cretaceous Bluesky Formation, Alberta, Canada. Journal of Sedimentary Research, 81, 901–920.

McAnally, W.H., Friedrichs, C., Hamilton, D., Hayter, E., Shrestha, P., Rodriguez, H., Sheremet, A., and Teeter, A., 2007, Management of fluid mud in estuaries, bays, and lakes. I: present state of understanding on character and behavior. Journal of Hydraulic Engineering, 133, 9–22.

Mossop, G.D. and Flach, P.D., 1983, Deep channel sedimentation in the Lower Cretaceous McMurray Formation, Athabasca Oil sands, Alberta. Sedimentology, 30, 493–509.

Musial, G., Reynaud, J.-Y., Gingras, M.K., Féniès, H., Labourdette, R., and Parize, O., 2012, Subsurface and outcrop characterization of large tidally influenced point bars of the Cretaceous McMurray Formation (Alberta, Canada). Sedimentary Geology, 279, 156–172.

Nardin, T.R., Feldman, H.R., and Carter, B.J., 2013, Stratigraphic architecture of a large-scale point-bar complex in the McMurray Formation: Syncrude's Mildred Lake Mine, Alberta, Canada. In: Hein, F.J., Leckie, D., Larter, S., and Suter, J.R. (eds.), Heavy-oil and Oil-sand Petroleum Systems in Alberta and Beyond. American Association of Petroleum Geologists Studies in Geology, 64, p. 273–311. https://doi.org/10.1306/13371583St643555

Plint, A.G., 2014, Mud dispersal across a Cretaceous prodelta: storm-generated, wave-enhanced sediment gravity flows inferred from mudstone microtexture and microfacies. Sedimentology, 61, 609–647.

Ranger, M.J. and Pemberton, S.G., 1997, Elements of a stratigraphic framework for the McMurray Formation in south Athabasca area, Alberta. In: Pemberton, S.G. and James, D.P. (eds.), Petroleum Geology of the Cretaceous Mannville Group, Western Canada. Canadian Society of Petroleum Geologists Memoir, 18, p. 263–291.

Ross, M.A. and Mehta, A.J., 1989, On the mechanics of lutoclines and fluid mud. Journal of Coastal Research, 5, 51–61.

Shinn, Y.J., Lee, H.S., Kwon, Y.K., and Kwak, W.J., 2014, Lithofacies distribution and depositional environment in the Lower Cretaceous McMurray Formation, BlackGold Lease, northern Alberta: implications for geometry and distribution of oil sand reservoirs. Geosciences Journal, 18, 325–337.

Soyinka, O.A. and Slatt, R.M., 2008, Identification and micro-stratigraphy of hyperpycnites and turbidites in Cretaceous Lewis Shale, Wyoming. Sedimentology, 88, 1117–1133.

Stockmal, G.S., Cant, D.J., and Bell, J.S., 1992, Relationship of the stratigraphy of the Western Canada foreland basin to Cordilleran tectonics: insights from geodynamic models. In: Macqueen, R.W. and Leckie, D.A. (eds.), Foreland Basins and Fold Belts. American Association of Petroleum Geologists Memoir, 55, p. 107–124.

Sumner, E.J., Talling, P.J., and Amy, L.A., 2009, Deposits of flows transitional between turbidity current and debris flow. Geology, 37, 991–994.

Traykovski, P., Geyer, W.R., Irish, J.D., and Lynch, J.F., 2000, The role of wave-induced density-driven fluid mud flows for cross-shelf transport on the Eel River continental shelf. Continental Shelf Research, 20, 2113–2140.

Wang, Z. and Larsen, P., 1994, Turbulent structure of water and clay suspensions with bed load. Journal of Hydraulic Engineering, 120, 577–600.

Wightman, D.M. and Pemberton, S.G., 1997, The Lower Cretaceous (Aptian) McMurray Formation: an overview of the Fort McMurray area, northeastern Alberta. In: Pemberton, S.G. and James, D.P. (eds.), Petroleum Geology of the Cretaceous Mannville Group, Western Canada. Canadian Society of Petroleum Geologists Memoir, 18, p. 312–344.

Yawar, Z. and Schieber, J., 2017, On the origin of silt laminae in laminated shales. Sedimentary Geology, 360, 22–34.